

PREDICTION OF FRACTURE INITIATION AT THREE-DIMENSIONAL BIMATERIAL INTERFACE CORNERS: APPLICATION TO BUTT-JOINTS LOADED IN BENDING

Paul E. W. Labossiere¹ and Martin L. Dunn²

¹Department of Mechanical Engineering, University of Washington, Seattle, WA

²Department of Mechanical Engineering, University of Colorado, Boulder, CO

ABSTRACT

Based on the universal nature of the asymptotic elastic fields at three-dimensional bimaterial interface corners, specifically that the stresses are singular with magnitude scaled solely by scalar stress intensities, we pursue the application of a fracture initiation criterion based on critical values of the stress intensities. To demonstrate this, we designed and fabricated a series of specimens consisting of two square aluminum prisms bonded together by a thin layer of epoxy. These butt-joint specimens were loaded in four-point flexure to failure. The orientation of the specimens was varied to encourage fracture to initiate at either the two-dimensional interface edge or the three-dimensional interface corner. We found that the failure stresses differ for each initiation mode, and depend significantly on the epoxy bond thickness. In order to apply the interface corner fracture initiation criterion, we carried out asymptotic calculations to determine the order of the stress singularity and the angular variation of the elastic fields at the interface corner. We determined the corresponding stress intensities, which depend on the far-field specimen geometry and loading, from full-field finite element calculations. From the measured failure stresses, we then determined the corresponding critical stress intensities. We found that although the failure stresses vary with epoxy thickness, the critical stress intensities do not, suggesting that they are a reasonable parameter to correlate fracture initiation.

KEYWORDS

Fracture Initiation, Bimaterial, Three-Dimensional, Interface Corner, Butt-Joint

INTRODUCTION

Consider the bimaterial interface corner geometry shown schematically in Figure 1. In general, the corner consists of intersecting faces (planes) and edges (lines) of arbitrary orientation. As shown, the edges may be *free* edges or *interface* edges. Each material, denoted by A and B , occupies a part of the solid and both materials may be anisotropic with principal material axes arbitrarily oriented with respect to the $(x\ y\ z)$ axes. We consider the faces to be traction free, although other homogeneous boundary conditions can be easily handled and the solid is loaded at remote boundaries by tractions and displacements.

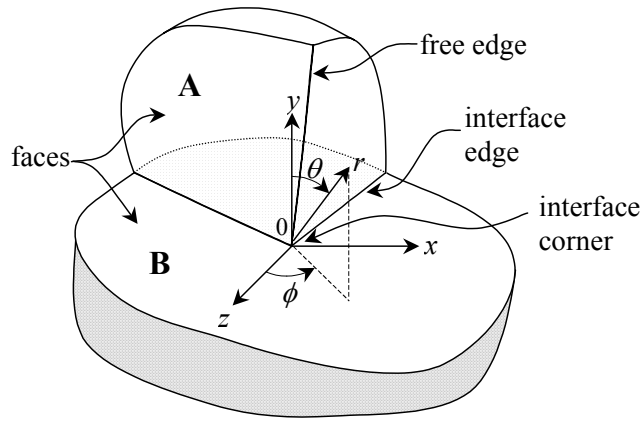


Figure 1: Three-dimensional bimaterial interface corner geometry showing coordinate axes. The faces (planes) and edges (lines) are arbitrarily oriented.

It is reasonably well known that a stress and a displacement field of the form [1-5]

$$\begin{aligned}\sigma_{ij}^M &= \sum_{m=-\infty}^{\infty} K_m^{3D} r^{\lambda_m-1} f_{ij}^{Mm}(\theta, \phi) \\ u_i^M &= \sum_{m=-\infty}^{\infty} K_m^{3D} r^{\lambda_m} g_i^{Mm}(\theta, \phi)\end{aligned}\quad (1)$$

exist in the region surrounding the tip of the three-dimensional bimaterial interface corner of Figure 1. In general, there are an infinite number of terms in the series, each corresponding to a specific deformation mode, m . Here λ_m-1 are the orders of the stress singularities, $f_{ij}^m(\theta, \phi)$ and $g_i^m(\theta, \phi)$ describe the angular variation of the stress and displacement fields in each material ($M = A, B$) and K_m^{3D} are the corresponding stress intensities. λ_m-1 , $f_{ij}^m(\theta, \phi)$ and $g_i^m(\theta, \phi)$ depend on the elastic mismatch and asymptotic interface corner geometry, and K_m^{3D} depend on the far-field loading and geometry. This expansion of the stress state is a natural generalization of the classical mode I, II and III fields in homogeneous isotropic cracked solids; however, the deformation modes generally do not possess the simple symmetry of cracks in homogeneous media. The deformation modes strongly depend on the elastic mismatch and the nature of the asymptotic corner geometry. In Eqn. 1, λ_m , $f_{ij}^m(\theta, \phi)$ and $g_i^m(\theta, \phi)$ can be determined from an asymptotic analysis of the stress state near the three-dimensional interface corner [2-5]. Note that $f_{ij}^m(\theta, \phi)$ may be singular along reentrant free edges and interface edges (see Figure 1). Only the stress intensities K_m^{3D} cannot be determined from the asymptotic analysis. They depend on the far-field geometry and loading of the solid.

Terms that give rise to both singular and nonsingular stresses exist in the series. Finite strain-energy at the three-dimensional bimaterial interface corner requires $\text{Re}\{\lambda\} > -1/2$ (for two-dimensional corners $\text{Re}\{\lambda\} > 0$) and finite displacements require $\text{Re}\{\lambda\} > 0$; however, as previously discussed [6,7] these are not completely satisfactory reasons for limiting the range of $\text{Re}\{\lambda\}$ since they are based on assessment of the elastic solution in a region where it is not valid. Very close to the interface corner the actual solution is usually perturbed by material nonlinearity and/or geometric perturbations from the ideal interface corner, and far from the interface corner, it is perturbed by the far-field boundaries and loads. The terms with eigenvalues in the range $0 < \text{Re}\{\lambda\} < 1$ may dominate the other terms in the series expansion of Eqn. 1 in an annular region surrounding the interface corner. In this annulus, these terms dominate higher-order singular terms because these have amplitudes that are small, and they dominate the nonsingular terms because the annulus is sufficiently close to the tip of the interface corner. Furthermore, in this elastic annulus the elastic fields for a particular loading mode exhibit a universal structure; their magnitude is simply scaled by a single parameter, the stress intensity K_m^{3D} . As such, this annulus is termed the K -annulus. The region where the higher-order singular terms are significant compared to the K_m^{3D} -term is embedded within

the K -annulus where material nonlinearities are likely to invalidate the elastic solution anyway. As in linear elastic fracture mechanics, K_m^{3D} is a measure of how the far-field load and geometry are communicated to the interface corner. Thus for a given material pair and three-dimensional bimaterial interface corner geometry, the asymptotic elastic fields are completely characterized by K_m^{3D} . For these reasons, we consider only values in the range $0 < \text{Re}\{\lambda\} < 1$; the results for the geometry and loads considered here show that for the analysis of fracture initiation, these terms are sufficient. We caution, however, that for other geometry and load cases, this may not be the case.

In practice, an interface corner can be the site of fracture initiation because of the existence of highly elevated stresses. Technological examples include microelectronics and microsensor packaging where interfaces arise due to various bonding and encapsulating processes that inevitably result not only in multimaterial interfaces, but also in multimaterial free edges and corners which are site of potential interface failure [8]. Given the universal nature of the stress field near the three-dimensional bimaterial interface corner, which is scaled by the three-dimensional stress intensities, a reasonable approach to correlate fracture initiation appears to be the use of critical values of the stress intensities. Specifically, in the spirit of Irwin for classical linear elastic fracture mechanics, we pursue a fracture initiation criterion of the form $f(K_m^{3D}) = f_{cr}$. This criterion says fracture will initiate at the three-dimensional interface corner when some combination of K_m^{3D} reaches a critical value. The criterion only addresses initiation; the subsequent crack propagation is a related, but different problem. In general, the functional form of $f(K_m^{3D})$ and the critical value must be determined experimentally. The criterion can potentially be simplified to $K^{3D} = K_{cr}^{3D}$ if only one singular mode exists, as is the case for the interface corner geometry and material pair considered here or if one singularity dominates the effect of others (see for example Dunn et al., [9]). Further details regarding the approach presented here are given by Labossiere and Dunn [3]; they build heavily on similar ideas applied to two-dimensional situations. A comprehensive review of the use of critical stress intensities to correlate fracture initiation at two-dimensional bimaterial interface corners has recently been written by Reedy [10].

APPLICATION TO BUTT-JOINTS LOADED IN BENDING

We designed and fabricated a series of butt-joint test structures with three-dimensional bimaterial interface corners composed of 6061-T6 aluminum and cast West System 105-205 epoxy. Both materials are isotropic with $E = 70.0$ GPa and $\nu = 0.33$ for the aluminum and $E = 2.98$ GPa, $\nu = 0.38$, and $\sigma_y = 52$ MPa for the epoxy. A schematic of the test structures and the load configuration is shown in Figure 2. The structures are prisms with a square cross section and an overall length of 150 mm. The butt-joint of thickness a ranging from 0.05 to 1.1 mm is located in the center of the specimen, and the bimaterial interface is square with dimensions $w \times w$, where $w = 25.4$ mm. The specimens are loaded in four-point flexure in the $-x$ -direction of Figure 3 with $L = 127$ mm and $l = 76.2$ mm. The load and supports are symmetrically located with respect to the butt-joint. A similar set of experiments was performed on two-dimensional specimens which were identical in geometry; however, the specimens were rotated 45 degrees about the z -axis in Figure 2, forcing fracture initiation to occur at the bottom interface *edge*, making the geometry and loading two-dimensional. This specimen geometry and load configuration was chosen for several reasons: four-point flexure loading is relatively simple to perform; fracture initiation occurs at one of the interface *corners* on the bottom of the specimen; by introducing only one finite length scale, a , the analysis is simplified, and; there is only one eigenvalue $\lambda=1$ giving rise to singular stresses at the three-dimensional bimaterial interface corner, which also simplifies the analysis and interpretation of the results.

The specimens were prepared as follows: The surfaces of the aluminum prisms to be bonded were machined flat and subsequently polished with 1500 grit paper and cleaned in 1-1-1 Trichloroethane, the aluminum prisms were placed in a mold coated with a wax release film and the epoxy was cast

within 20 minutes of the cleaning process. Once the epoxy cured at room temperature, the specimens were carefully removed and then wet polished to reveal well-defined interface corners and interface edges. The radius of curvature of the three-dimensional aluminum/epoxy interface corners was measured with optical microscopy and in all cases was less than 8 μm .

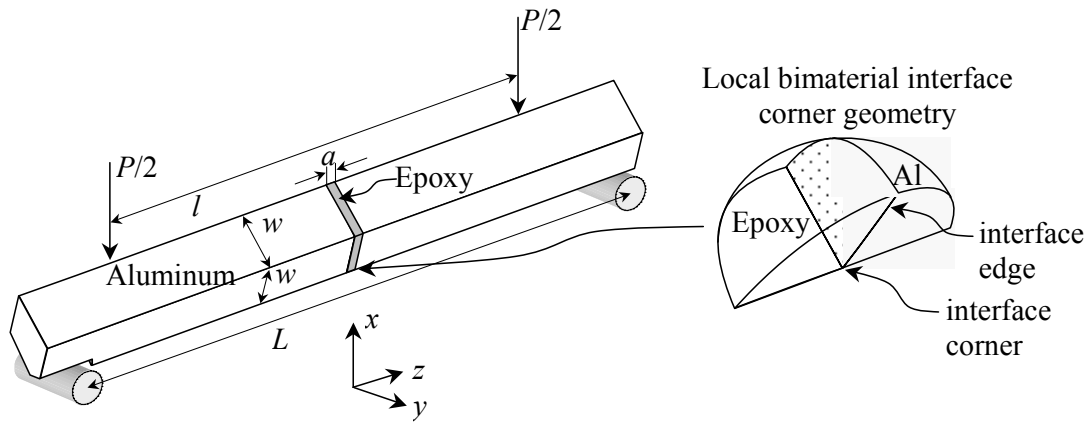


Figure 2: Four-point flexure test set-up showing butt-joint specimen dimensions and local three-dimensional bimaterial interface corner geometry.

The result of asymptotic calculations show that there is a stress singularity of order $\lambda-1 = -0.351$ at the three-dimensional aluminum/epoxy interface corner and a stress singularity of order $\lambda-1 = -0.292$ along the two-dimensional interface edges. The complete structure of the near tip fields for this geometry and material pair can be found in Labossiere and Dunn [3]. Dimensional considerations dictate that the stress intensity K^{3D} for the three-dimensional interface corner geometry considered here takes the form:

$$K^{3D} = \sigma_o^{3D} a^{1-\lambda} Y^{3D} \left(\frac{E_A}{E_B}, \nu_A, \nu_B \right). \quad (2)$$

Here a is the epoxy thickness, and σ_o^{3D} is the normal stress that would exist at the bottom tip of a homogeneous beam of dimension $w \times w$ under the four-point flexure loading of Figure 2:

$$\sigma_o^{3D} = \frac{3P(L-l)}{\sqrt{2}w^3}. \quad (3)$$

In general, Y^{3D} is a nondimensional function of both the elastic mismatch (E_A, E_B, ν_A , and ν_B are the Young's moduli and Poisson's ratios of the two materials) and the geometry, however, by designing our specimens with only one finite length scale a , the effect of geometry appears solely through $a^{1-\lambda}$, and Y^{3D} becomes a function of elastic mismatch only. Furthermore, since the elastic mismatch is fixed for the aluminum/epoxy material pair considered here, Y^{3D} is a constant. We determined Y^{3D} from detailed full-field finite element analyses of the three-dimensional aluminum/epoxy specimens loaded in four-point flexure using a commercially available finite element code. Typical finite element models contained ~ 100000 degrees of freedom with highly refined meshes near the interface corner to ensure accurate modeling of the asymptotic elastic fields. Y^{3D} was obtained from the finite element results by matching the finite element solution for the displacements near the interface corner with the asymptotic displacements of Eqn. 1 along certain rays emanating from the bimaterial interface corner using a least squares approach. Calculations for various epoxy thicknesses over the range being tested showed that Y^{3D} is indeed a constant and its value is $Y^{3D} = 0.431$. Although not presented here, similar analyses were performed for the two-dimensional specimen geometry.

MECHANICAL TESTING AND INTERPRETATION OF THE RESULTS IN TERMS OF CRITICAL STRESS INTENSITIES

Mechanical fracture testing was carried out using the four-point flexure configuration shown in Figure 2. A servo-hydraulic mechanical test system was used to load the specimens under load-point displacement control at a rate of 0.01 mm/sec. In all the tests, the load-displacement response was linear until brittle fracture occurred. The brittle fracture is characterized by a crack that initiated at one of the aluminum/epoxy interface corners on the tensile side of the specimen followed by unstable crack propagation along the interface. This is unlike *tougher* interfaces where the crack may kink away from the interface and run into one of the adherends (see for example Dunn et al., [9]).

Figure 3 shows the measured failure stresses calculated using Eqn. 3 plotted as a function of epoxy thickness a . Note that the measured failure stress depends strongly on the epoxy thickness invalidating its use as a failure criterion. The critical stress intensity criterion is applied by substituting into Eqn. 2, the measured specimen dimensions and failure stresses to calculate the corresponding critical values of the stress intensities. The critical stress intensities so obtained do not show a systematic variation with epoxy thickness suggesting they are universal parameters that can be used to correlate fracture initiation. The solid line of Figure 3 denotes the predicted failure stress based on the critical stress intensity fracture initiation criterion $K^{3D} = K_{cr}^{3D} = 6.6 \text{ MPa mm}^{0.35}$. It accurately describes the variation of the measured failure stresses with epoxy thickness a . Although the results for the two-dimensional interface corner butt-joint specimens are not presented in detail here, the critical stress intensities also do not show a systematic variation with the geometry and the variation of the measured failure stresses with epoxy thickness is accurately described by the critical stress intensity fracture initiation criterion $K^{2D} = K_{cr}^{2D} = 4.4 \text{ MPa mm}^{0.29}$. Note that the strength of the stress singularity is different in this case, thus the units of the corresponding stress intensity are also different as is the variation in the measured failure stress with epoxy thickness.

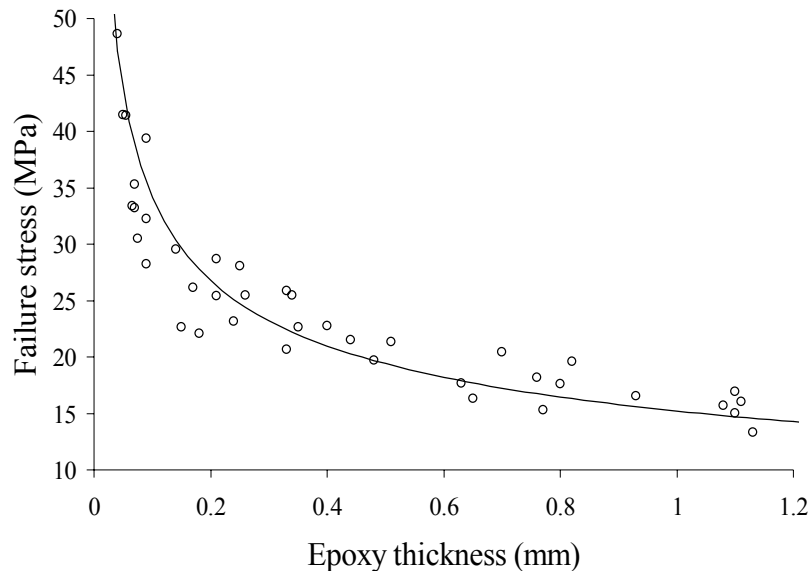


Figure 3: Measured failure stress versus epoxy thickness. The solid line is the prediction based on a constant critical stress intensity of $K_{cr}^{3D} = 6.6 \text{ MPa mm}^{0.35}$.

The success of the critical stress intensity failure criterion requires that the elastic asymptotic solution of Eqn 1 accurately describes the actual solution in some region surrounding the interface corner where fracture initiation occurs. The size of the region in which the asymptotic solution accurately approximates the full-field solution obtained from finite element calculations (within ten percent error) as measured along the ray bisecting the aluminum/epoxy interface is roughly 0.014mm for the specimens with the thinnest epoxy layer ($a = 0.05\text{mm}$) and 0.3mm for the thickest epoxy layer ($a = 1.1\text{mm}$). We also examined the region of dominance along other rays emanating from the bimaterial

interface corner on the interface and in all cases, the region of dominance is larger along any other ray. Although this is relatively small compared to the specimen size, it is larger than the finite corner radius, which is less than 8 μm . It is also larger than any plastic zone size, which can be estimated using the von Mises yield criterion applied to the elastic asymptotic solution for the three-dimensional interface corner and is on the order of 2 μm [3]. Thus the correlation of fracture initiation based on a critical value of $K^{3D} = K_{cr}^{3D}$ seems reasonable.

CONCLUSIONS

We demonstrated an approach to characterize fracture initiation at three-dimensional bimaterial interface corners using critical values of the stress intensities that arise in a linear elastic analysis. We designed and fabricated a series of two-dimensional and three-dimensional aluminum/epoxy/aluminum butt-joint specimens with interface edges and corners, respectively. We mechanically loaded them to failure in four-point flexure. The measurements produced a critical nominal load (critical nominal stress), but these varied significantly with bond thickness and thus invalidated their use as critical values to correlate fracture initiation. From a rigorous analysis of the interface corner stress state, we determined the order of the stress singularity, the angular variations of the stress and displacement fields, and the corresponding stress intensity for the specified loading. The critical stress intensities obtained from the failure loads did not show a systematic variation with adhesive thickness, a feature suggestive of the universal nature of the criterion.

REFERENCES

1. Williams, M. L. (1952) *J. Appl. Mech.*, 19, 526-528.
2. Bazant, Z. P. (1974) *Int. J. Engng Sci.*, 12, 221-243.
3. Labossiere, P. E. W., and Dunn, M. L., (2001) *J. Mech. Phys. Solids*, Vol. 49, 609-634.
4. Ghahremani, F. (1991) *Int. J. Solids Structures*, Vol. 27, 1371-1386.
5. Picu, C. R. and Gupta, V. (1997) *J. Mech. Phys. Solids*, 45, 1495-1520.
6. Hui, C. Y., and Ruina, A. (1995) *Int. J. Fract.*, Vol. 72, 97-120.
7. Dunn, M. L., Hui, C. Y., Labossiere, P. E. W., and Lin, Y. Y., (2001) *Int. J. Fract.*, in press.
8. Chen, W. T., Read, D., Questad, D., and Sammakia, B. (1997) *Application of Fracture Mechanics in Electronic Packaging, ASME, AMD-Vol. 222/EEP-Vol. 20*, 183-192.
9. Dunn, M. L., Cunningham, S. J., and Labossiere, P. E. W. (2000) *Acta Materialia*, 48, 735-744.
10. Reedy, E. D., 2001, Strength of Butt and Sharp-Cornered Joints, *Comprehensive Adhesion Science*, in press.